Probabilistic prediction of SPI categories in Iran using sea surface temperature climate indices

Amin Shirvani[a*] and Willem A Landman[b]

[a] Department of Water Engineering, Oceanic and Atmospheric Research Center, College of Agriculture, Shiraz University, Shiraz, Iran.

[b] Department of Geography, Geoinformatics and Meteorology, University of Pretoria, Pretoria, South Africa.

Abstract

This study examines probabilistic prediction of the standardized precipitation index (SPI) categories (i.e., dry, normal and wet conditions) in Iran regressed onto the combination of the North Atlantic Oscillation (NAO) index and several sea-surface temperature (SST) indices including Niño4, Niño3.4, Niño3, Niño1+2, western Pacific (WP; 0º-15ºN, 130Eº-160ºE), the eastern Mediterranean Sea (EM; 30ºN-38ºN, 20ºE-35ºE) and the Indian Ocean Dipole (IOD). The ordinal regression models (ORM) based on the logistic function are applied to determine the best predictor variables. Seasonal precipitation during the two wet seasons of October-December (OND) and January-March (JFM) for 50 synoptic stations across Iran for the period 1967-2017 are used in this research. 3-month SPI at the end of December and March, which provides SPI values over OND and JFM, is constructed based on the Gamma probability distribution. The SPI categories for OND and JFM precipitation averaged over Iran are considered as the predictand variables in the ORM. The linear trend analysis of JFM SPI values indicates that the risk of drought has been enhanced in this season. Among all individual predictors, the SST anomalies over the central Pacific Ocean has the strongest teleconnection with OND SPI categories. Based on the minimum Akaike information criterion (AIC), the combination of Niño3.4 and WP gives the best model for probabilistic prediction of wet and dry events in OND. Unlike the OND, the SST anomalies over different parts of the Pacific Ocean are not strongly related to the SPI values of the JFM season in Iran. Among all indices, only the SST anomaly variations over the eastern Mediterranean Sea are statistically teleconnected to JFM SPI categories and can be used to predict dry and wet events probability in Iran.

Key Words Climate indices, SST anomalies, SPI categories, Prediction.

[*] Corresponding author's email addresses: am_shirvani@hotmail.com; ashirvani@shirazu.ac.ir.

1. Introduction

The El Niño-Southern Oscillation (ENSO) phenomenon is a well-known variable climate mode which impacts on the seasonal climate variability across the planet (Mason and Goddard 2001) . The teleconnection between ENSO and precipitation variability has been studied in various regions of the world (e.g., Northern Arabian/Persian Gulf: (Al Senafi and Anis 2015); Iran: (Alizadeh-Choobari et al. 2018; Nazemosadat and Ghasemi 2004); Saudi Arabia: (Athar 2015); southwest Asia: (Barlow et al. 2002); northwest Indian Ocean: (Hoell et al. 2014a); northern hemisphere: (Hoell et al. 2014b); Mediterranean region: (Krichak et al. 2014); southwest central Asia: (Mariotti 2007); UAE: (Niranjan Kumar and Ouarda 2014); Israel: (Price et al. 1998); central southwest Asia: (Syed et al. 2006); east Asia and central Asia: (Yin et al. 2014)). ENSO has a large contribution in seasonal forecast skill (Balmaseda and Anderson 2009; Goddard and Dilley 2005; Landman and Beraki 2012; Weisheimer et al. 2009; Shirvani and Landman 2016). It has also been found that the seasonal prediction skill level is dependent on the strength of the teleconnection between ENSO and seasonal variability (Landman et al. 2019). Seasonal precipitation predictability over Iran is mainly restricted to October-December (OND) when ENSO states are strongly linked to Iranian precipitation variability (Shirvani and Landman 2016).

Raziei et al. (2012) studied the relationship between daily mean 500 hPa geopotential height fields and the occurrence of winter dry/wet spells in western Iran. They reported that wet events in central and southwestern Iran are related to the occurrence of a deep and large trough over the eastern Mediterranean Sea and the Red Sea, while dry conditions tend to be related to a ridge located over Turkey and the Balkans. Zarei et al. (2017) applied Markov chain models to monitor and predict SPI classes time series in Iran. They showed that in most synoptic stations, normal, moderately dry, and severe dry classes of drought have the highest frequency of occurrence. SPI values time series in the Karkheh river basin in Iran have been predicted using auto-regressive integrated moving average (ARIMA) models (Karimi et.al. 2019).

The occurrence of two severe droughts over the Middle East and central south Asia during 1998-2001 and 2007-2008 were associated with La Niña conditions and warm sea-surface temperature (SST) over the western Pacific (Agrawala et al. 2001; Barlow et al. 2002; Hoell et al. 2012; Hoell et al. 2014a). Another drought, during November 2013–April 2014, over an area extending from the Mediterranean coastal Middle East, northward through Turkey and eastward through Kazakhstan, Uzbekistan, and Kyrgyzstan, was also associated with La Niña conditions and warm SST over the western Pacific (Barlow and Hoell 2015). The teleconnection between ENSO and precipitation during January-March (JFM) over Iran is weak, but it is strong during OND (Nazemosadat and Cordery 2000; Nazemosadat and Ghasemi 2004; Shirvani and Landman 2016). The impact of central Pacific El Niño on the annual precipitation in Iran is not statistically significant, but both La Niña and the eastern El Niño impacts significantly on the annual precipitation (Alizadeh-Choobari et al. 2018). Rana et al. (2018) reported that much of seasonal precipitation predictability over the central southwest Asia (CSWA) during November-April is from preceding (September-October) SST variations in the Pacific related to ENSO and the Pacific decadal oscillation (PDO). These studies indicate that precipitation variability over the Middle East and CSWA can be modelled by using SST climate indices. In the present study, the combination of several SST climate indices- including Niño4, Niño3.4, Niño3, Niño1+2, western Pacific, eastern Mediterranean Sea and the Indian Ocean Dipole (IOD)- and the North Atlantic Oscillation

(NAO) are considered to predict the standardized precipitation index (SPI) categories (i.e., dry, normal and wet conditions) in Iran. Ordinal regression models (ORM) are examined here for the probabilistic prediction of dry, normal and wet categories using these SST indices. The ORM have been employed to characterize drought categories in U.S. Drought Monitor based on several drought indices (Hao, 2016). The other classifier models, such as artificial neural network (ANN) and support vector machine (SVM; Bazrkar and Chu, 2022), can be employed for drought prediction. The prediction skill of these models is generally higher than regression models. However, the interpretation and explanation of relationships between predictor variables and drought, based on these models, is not straightforward. Moreover, probabilistic drought prediction, which has been popular for decision making when the skill of drought prediction is low (Demargne et al., 2014), is not the target variable in these models. The predictability of SPI categories over Iran has not been studied before. The ORM are separately developed for two wet seasons (OND as autumn and JFM as winter) because their seasonal variability in response to SST over the Pacific Ocean, Indian Ocean and eastern Mediterranean Sea differs, unlike previous studies (Barlow and Hoell 2015; Rana et al. 2018; Barlow et al. 2021) that considered November-April as a single season. The main goal of this work is to identify and model the important factors which impact on dry and wet conditions in OND and particularly in JFM season, while the teleconnections between JFM precipitation over Iran with SST over the Pacific Ocean is weak.

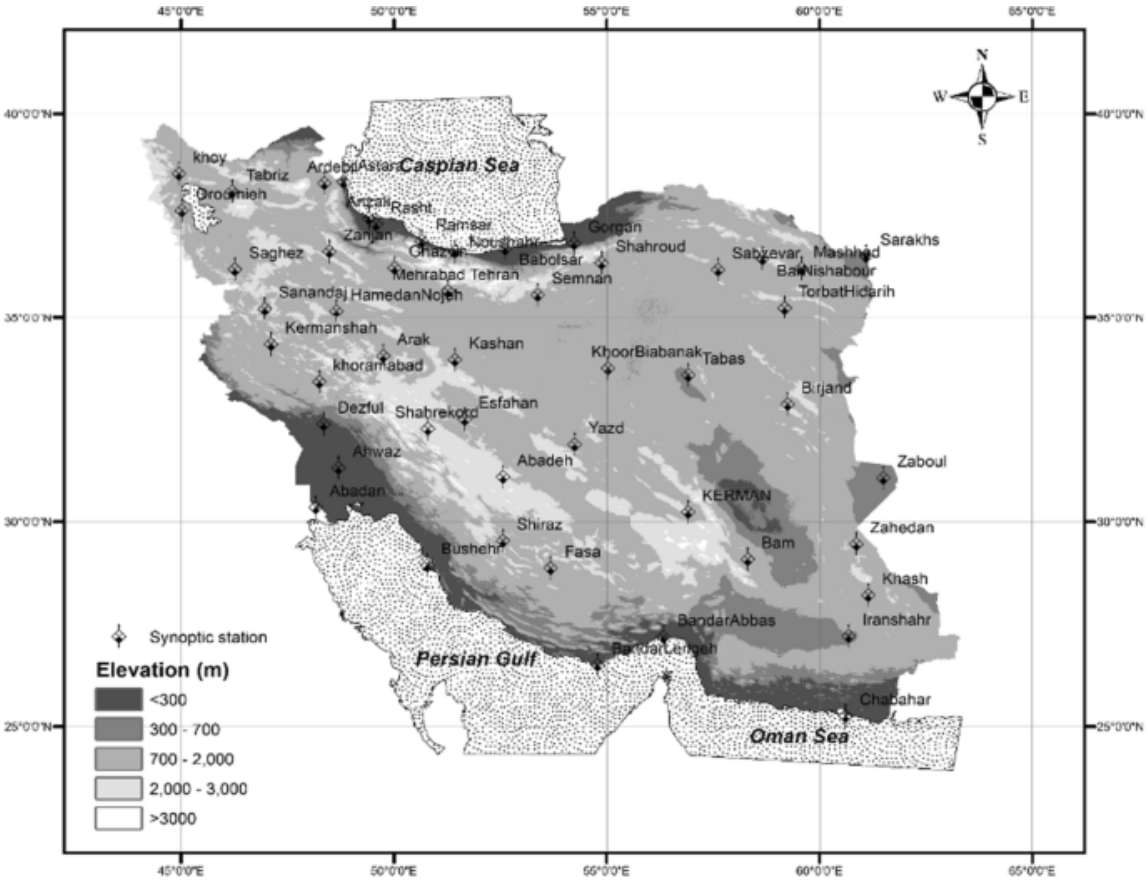

Figure 1. The geographical location of the synoptic stations

2. Datasets

2.1. Observed precipitation data

The monthly precipitation data for fifty synoptic stations are extracted from the website of the Islamic Republic of Iran Meteorological Office (IRIMO, http://www.irimo.ir/). The precipitation data set is quality controlled by the IRIMO. Figure 1 indicates the geographical locations of the selected stations over Iran. In this study, OND (as autumn season) and JFM (as winter season) time series precipitation data are studied for the two 50-year periods of 1967-2016 and 1968-2017, respectively. These seasons are two main rainy seasons in Iran such that about 60% of the annual precipitation over Iran occurs in these seasons, based on the IRIMO data for the period 1967-2017. Like the works of Hoell et al. 2014b, Hoell et al. 2015 and Barlow et al. 2021, which studied the area averaged over the Middle East, the spatial average of synoptic stations in Iran is considered for prediction of dry, normal and wet events in Iran.

2.2. SST data

The monthly NOAA Extended Reconstructed sea-surface temperature anomalies (SSTA) version 5 (ERSST) at a 2°×2° spatial resolution (Huang et al. 2017) are extracted from the International Research Institute (IRI) for Climate and Society (http://iridl.ldeo.columbia.edu/) for the period 1967-2017. SST anomalies over the 50 years for the OND and JFM seasons are then constructed over the western Pacific (WP) (SSTA averaged over 0º-15ºN, 130Eº-160ºE) and eastern Mediterranean Sea (EM) (SSTA averaged over 30ºN-38ºN, 20ºE-35ºE).

Also, several established climate indices including the Niño3 index (SSTA averaged over 5ºS-5ºN, 150ºW-90ºW), Niño3.4 index (SSTA averaged over 5ºS-5ºN, 170ºW-120ºW; which representing the central part (CP) ENSO influence), Niño4 index (SSTA averaged over 5ºS-5ºN, 160ºE-150ºW), Niño1+2 index (SSTA averaged over 10ºS-0º, 90ºW-80ºW; which representing the eastern part (EP) ENSO influence), North Atlantic Oscillation (NAO), Indian Ocean Dipole (IOD) are simultaneously examined as the candidate predictors in regression models to identify their respective influences on seasonal precipitation variability over Iran. These SST climate indices and the following reanalysis data are also extracted from the IRI data library.

2.3. Reanalysis specific humidity, winds data and mean sea level pressure

Monthly reanalysis specific humidity (q), zonal (u) and meridional (v) components of winds are taken from the NCEP-NCAR reanalysis data (Kalnay et al. 1996). This study uses these variables to calculate vector wind and precipitable water (PW; column-integrated water vapour amount). The PW is defined as the total atmospheric water vapour contained in a vertical column from the surface to the specified height in the atmosphere (Glickman, 2000). In the present study, the PW is considered as the integrated total atmospheric water vapour from the surface to the top of the atmosphere. The units of PW and wind components are kgm^{-2} and ms^{-1}, respectively.

3. Methods

The standardized precipitation index (SPI) (McKee et al. 1993) is applied to drought monitoring around the world and recommended by WMO (Svoboda et al. 2012). Table 1 which is available from WMO library (https://library.wmo.int/pmb_ged/wmo_1090_en.pdf) shows the SPI value classification system which is used to

define dry and wet conditions, including drought intensities. This classification system is used here to define dry and wet conditions. According to Table 1, those SPI values which are less (more) than -1 (+1) are considered here as the dry (wet) condition. The dry and wet conditions are also obtained from the percentiles of the SPI values. Three month SPI at the end of December and March is considered in this study. This time scale provides SPI values over OND and JFM. The 3-months SPI values for both OND and JFM based on the Gamma probability distribution are constructed.

Table 1. SPI classification

2.0+	Extremely wet
1.5 to 1.99	Very wet
1.0 to 1.49	Moderately wet
– 99 to 0.99	Near normal
– 1.0 to – 1.49	Moderately dry
– 1.5 to – 1.99	Severely dry
– 2 and less	Extremely dry

The linear trend and Mann- Kendall test, respectively, as the parametric and nonparametric methods are employed to investigate the properties of the trend in SPI values and SSTA. The assumption of the regression models is that the data series have no statistically significant trend. In the regression models, the assumption of stationary in the mean helps to understand the relationship between the fluctuation of predictors and predictand. If a series has a significant linear trend, then this series is not stationary in the mean and a de-trended series using the corresponding fitted linear trend is utilized before constructing the ordinal regression models to be used here. The SPI categories have a natural ordering to their classes such that low, normal, and high precipitation amounts can be classified using categories of dry, normal and wet. These categories can be arranged so that $category\ 1\ (dry) < category\ 2\ (normal) < category\ 3(wet)$ represent the scale of the precipitation amount. The cumulative probabilities for these categories are modeled using an ordinal regression model through logit transformation. The cumulative probabilities for category j of SPI is

$$P(SPI\_Cat \leq j) = \pi_1 + \pi_2 + \pi_j, \qquad for\ j = 1, 2,\ 3, \tag{1}$$

where π_j is the probability for category j ($P(SPI\_Cat = j) = \pi_j$),$P(SPI\_Cat \leq 0) = 0,\ and\ P(SPI\_Cat \leq 3) = 1$. The summation of probabilities for three categories is equal to one ($\pi_1 + \pi_2 + \pi_3 = 1$). Therefore, the following equations are expressed only for categories 1 and 2 because the probability for category 3 can be calculated from the summation of probabilities for categories 1 and 2 ($\pi_3 = 1 - \pi_1 - \pi_2$). Ordinal regression models can examine the effect of predictor variables $X_1, X_2, \ldots, X_p$ (e.g.,) on the log-odds of SPI categories cumulative probabilities,

$$logit[P(SPI\_Cat \leq j)] = \log\left[\frac{P(SPI\_Cat \leq j)}{1 - P(SPI\_Cat \leq j)}\right] = \log\left[\frac{\pi_1 + \cdots + \pi_j}{1 - (\pi_1 + \cdots + \pi_j)}\right],\ j = 1,2. \tag{2}$$

As ordinal regression model for predicting these logits cumulative can be written as

$$logit[P(SPI\_Cat \leq j)] = \alpha_{j0} + \beta_1 X_1 + \beta_2 X_2 + \cdots + \beta_p X_p,\quad j = 1,2. \tag{3}$$

Probabilities for a particular SPI categories j are obtained by

$$\pi_1 = P(SPI\_Cat = 1) = P(SPI\_Cat \leq 1), \quad (4)$$

$$\pi_2 = P(SPI\_Cat = 2) = P(SPI\_Cat \leq 2) - P(SPI\_Cat \leq 1), \quad (5)$$

and

$$P(SPI\_Cat \leq j) = \frac{\exp(\alpha_{j0}+\beta_1 X_1+\beta_2 X_2+\cdots+\beta_p X_p)}{1-\exp(\alpha_{j0}+\beta_1 X_1+\beta_2 X_2+\cdots+\beta_p X_p)}, \quad j = 1,2 \quad (6)$$

More details for ordinal regression models can be found in statistical texts such as (Bilder 2014). In the present study, the $polr$ function from the $MASS$ R package is used for parameters estimation using the maximum likelihood method. The logistic method is applied to perform the logit transformation in the $polr$ function. The surrogate approach (Liu and Zhang 2018) is applied to residual diagnostic for validating the ordinal regression assumptions. The surrogate approach is implemented using the $SURE$ package in R software. The ordinal regression model that gives the minimum Akaike Information Criterion (AIC) and follows the assumptions of residual independence is selected as the best model. The cross validation (Wilks 2011) ordinal regression model using a one-year-out window is applied for evaluating the selected model. The confusion matrix is computed to show the performance of the cross validation ordinal regression model.

4. Results and Discussions

4.1. Trend analysis of SPI values over Iran

The p-value of the one sample Kolmogorov-Smirnov (KS) test based on the Gamma distribution for OND (JFM) precipitation data is 0.6 (0.42), indicating that seasonal precipitation follows a Gamma distribution. The KS test p-value is 0.001 for a Normal distribution for both seasons, indicating that the Normal distribution is not appropriate for seasonal precipitation data over Iran. So, the SPI values of OND and JFM precipitation time series are subsequently computed based on the Gamma distribution. The SPI values time series for OND and JFM seasons are plotted in Fig. 2. The fitted linear regression for these times series were placed in this Figure. For example, the fitted linear regression equation for JFM season is expressed as follows.

$$SPI\_values(t) = -0.029 \times t + 58 + z_t, \qquad t = 1968,1983,\ldots,2017, \quad (7)$$

where the estimated slope $\hat{\alpha}_1 = -0.029$ with t-statistic and probability value of -3.2 and 0.002, indicating a significant downward trend at 5% significance level in SPI for the period 1968-2017. So, winter drought index over Iran has decreased about -1.4 during the last five decades. The applied linear regression for OND SPI time series indicates a non-significant trend at the 5% significance level (Table 2). Figure 2 (b) and Table 2 indicate that the JFM SPI values have significantly decreased over Iran based on observed precipitation data. However, autumn (OND) drought index over Iran does not have a statistically significant trend. The nonparametric Mann-Kendall test also confirms these results (Table 2).

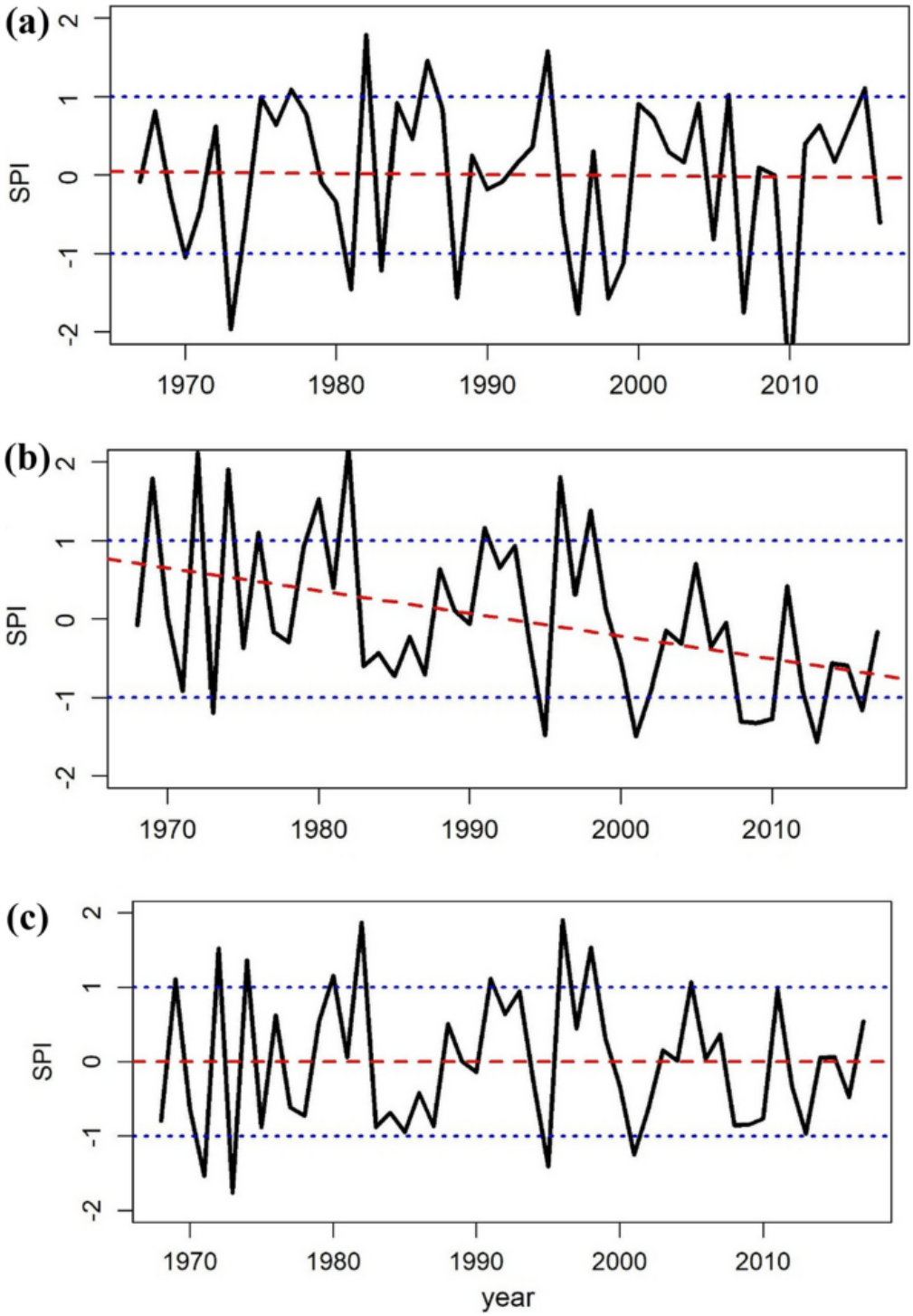

Figure 2. Time series plot of OND (**a**), JFM (**b**) and JFM de-trended (**c**) SPI values. The red dash lines show the corresponding linear trends. The horizontal blue dot lines show thresholds for dry and wet conditions

Table 2. The estimated parameters of linear trend and MK tests for OND and JFM for the periods 1967–2016 and 1968–2017, respectively

	Simple linear regression			Mann–Kendal	
Seasons	Slope	*t* value	*P* value	*z*	*p* value
OND	− 0.001	− 0.14	0.88	0.03	0.97
JFM	− 0.029	− 3.2	0.002**	− 2.7	0.006**

**indicates significant trend at 1% significance levels

If a time series has a significant linear trend, then this series is not stationary in the mean. In constructing statistical relationships between predictors and predictand variables, the assumption of stationary in mean helps to extract the relationship between the fluctuations of predictors and predictand. Before constructing ordinal regression models, the de-trended JFM SPI time series are obtained using the abovementioned fitted linear regression and plotted in Fig. 2 (c). This de-trended SPI time series is considered for SPI categories. Also, if a significant linear trend is observed in the predictor variables (e.g., OND WPSSTA and JFM EMSSTA), a de-trended series is utilized before performing ordinal regression models.

4.2. Fitted models for SPI categories

The specified SPI categories (i.e., dry, normal and wet conditions) according to classification system in Table1 are consistent with classifying based on the percentiles of the SPI values such that dry and wet conditions are the lower and upper 20th and 80th percentile of the SPI values. This ordinal variable (i.e., SPI categories) is considered as the predictand (or response) variable in ordinal regression models. The SST climate indices described above are combined as the predictor variables in these models. After removing the non-significant variables among predictors and performing backward stepwise regression, the following ordinal regression model with minimum values of AIC (68.3) and residual deviance (60.3) is the best model for predicting the OND SPI categories.

$$logit\big(P(OND\_SPI\_CAT \le j)\big) = \hat{\alpha}_{j0} - 1.15OND_{Niño3.4} + 5.25{OND_{WPSSTA}}^{d}, \quad j = 1,2 \qquad (8)$$

or

$$P(OND\_SPI\_CAT \le j) = \frac{\exp\big(\hat{\alpha}_{j0} - 1.15OND\_Niño3.4 + 5.25OND\_WPSSTA^{d}\big)}{1 + \exp\big(\hat{\alpha}_{j0} - 1.15OND\_Niño3.4 + 5.25OOND\_WPSSTA^{d}\big)}, \quad j = 1,2 \qquad (9)$$

where $\hat{\alpha}_{10}$=-2.1 and $\hat{\alpha}_{20}$=3.4 . The d superscript in OND_WPSSTA indicates de-trended series. The standard error of the estimated coefficients $OND\_Niño3.4$ and OND_WPSSTA^{d} are, respectively, 0.42 and 2.25, indicating the corresponding t statistic values are $\frac{-1.15}{0.42} = -2.7$ and $\frac{5.25}{2.25} = 2.3$ which are greater than the quintile of the t-distribution with alpha=0.05 (i.e., t= 1.96). Also, the corresponding p-values are 0.002 and 0.012 and therefore, the estimated coefficients are statistically significant at 5% significance level. So, there is sufficient statistical evidence that SSTA over the central and eastern parts of the Pacific Ocean are important factors for predicting OND SPI categories over Iran because of the significant and large t statistic values for these predictors. Moreover, the association between OND SPI categories and $OND\_Niño3.4$ in comparison with OND_WPSSTA^{d} is in an opposite direction. This result suggests that the SSTA over the tropical Pacific Ocean act as a dipole in predicting OND SPI categories.

The autocorrelation function of the model's surrogate residuals was plotted in Fig. 3a and used to test if the surrogate residual time series are serially correlated. Figure 3a indicates that the correlation coefficients at all lags are not statistically significant at 5% significance level and therefore, surrogate residual series are not serially correlated. The scatter plots of surrogate residual and $OND\_Niño3.4$ and OND_WPSSTA^d with fitted nonparametric curve plotted in Figs. 3b and 3c, which indicate no pattern between surrogate residual and individual predictor variables. Therefore, these assumptions, serially uncorrelated correlated surrogate residual and no relationship between surrogate residual and predictors, about the nature of the surrogate residual are met.

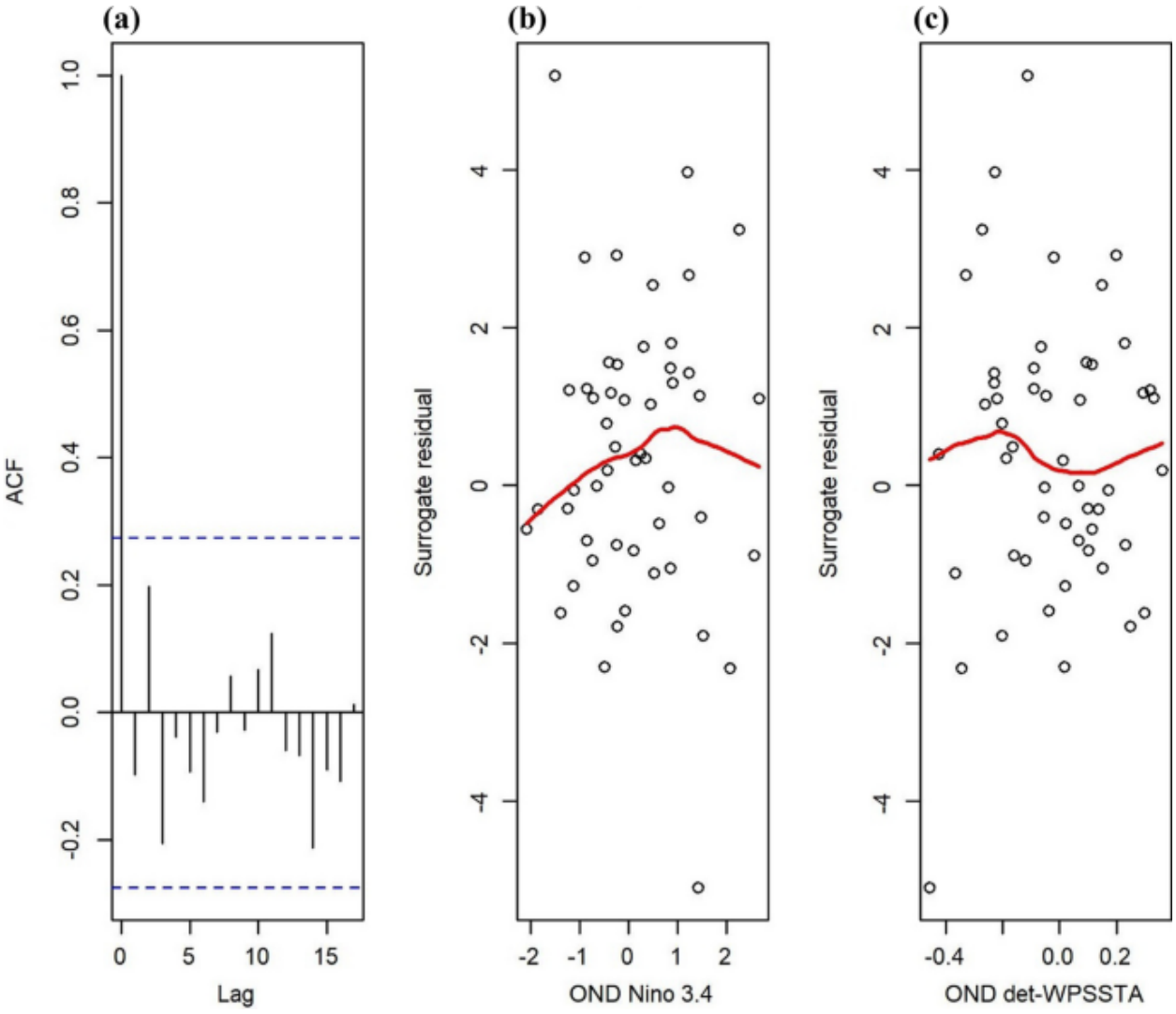

Figure 3. Autocorrelation function of the surrogate residuals (**a**); the dash lines indicate the confidence interval which is $\pm \frac{1.96}{\sqrt{n}}$. The scatter plots of surrogate residual and $ONDNiño3.4$ (**b**) and $OND.WPSSTA^d$ (**c**) with a nonparametric smooth (red curve)

The prediction of probabilities for each OND SPI category and year can be computed using equations (4-6). The estimated probabilities of SPI categories conditioned on the individual predictor variable (e,g., $OND\_Niño3.4$) are computed by holding the other predictor variable (e.g., OND_WPSSTA) as a constant value in the model for understanding of the role of the individual predictor variable in the model. Fig 4 shows plot of these estimated probabilities for individual predictor. The occurrence of dry (wet) OND season in Iran is high when SSTA over the central tropical Pacific Ocean are in the cold (warm) phase (Fig. 4a).

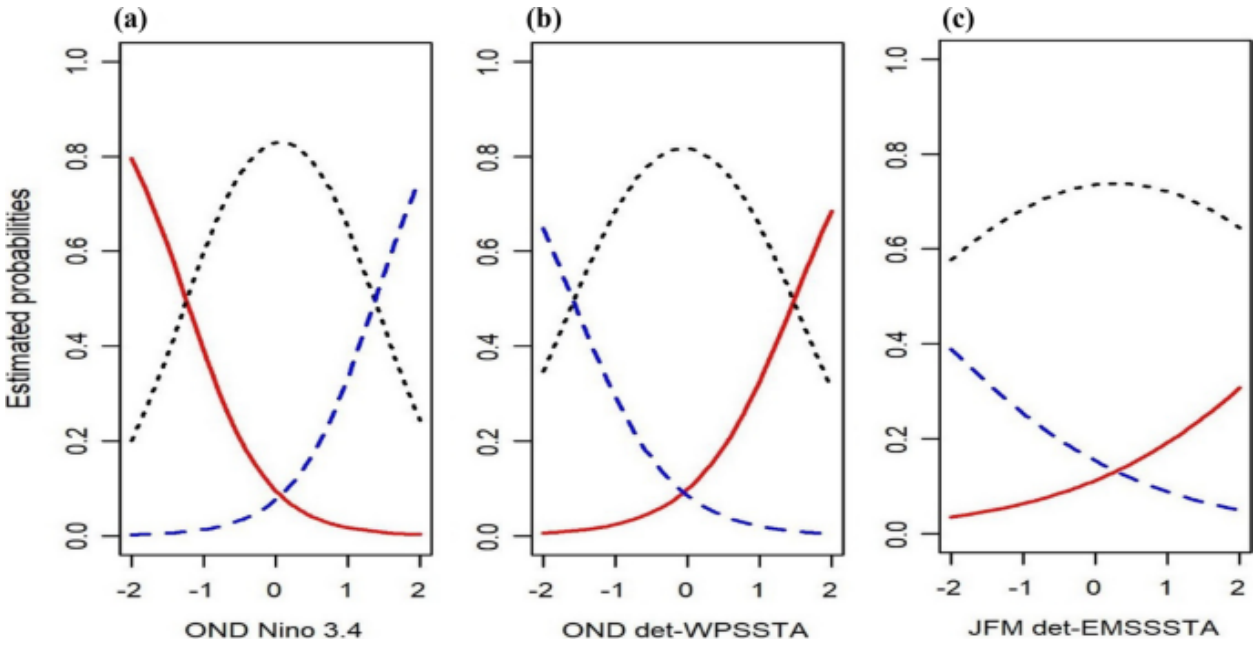

Figure 4. The estimated probabilities for individual predictor; $ONDNiño3.4$ (**a**), $OND.WPSSTA^d$ (**b**) and $JFM.EMSSTA^d$ (**c**). The red lines, black dots and blue dashes show dry, normal and wet conditions, respectively

The estimated coefficients, t statistic values and AIC of the fitted ordinal regression based on the individual predictor are presented in Table 3. All single predictor (except EM) are statistically significant at the 5% level for predicting OND SPI categories. However, among the individual candidate predictors, the best predictor is $ONDNiño3.4$ because of the maximum of t statistic value and minimum of AIC, which are -3.8 and 72.6, respectively. As two predictor variables are included in the ordinal regression models, both predictors in the following combinations (1) $OND\_Niño4$ and OND_WPSSTA^d, (2) $OND\_Niño3.4$ and OND_WPSSTA^d, (3) $OND\_Niño3$ and OND_WPSSTA, are significant at the 5% level. The corresponding AICs are 69.65, 68.33 and 71, respectively, indicating that the combination of OND_WPSSTA^d with $OND\_Niño3.4$ as predictors is the best of all the models. Also, combined predictors produce lower AIC than a single predictor. Moreover, these results indicate that SSTA variations over the western parts is an important factor in combination with $Niño$ indices for the prediction of OND SPI categories in Iran. These results are consistent with previous works (Agrawala et al. 2001; Barlow et al. 2002; Barlow and Hoell 2015; Hoell et al. 2012; Hoell et al. 2014a; Hoell et al. 2014b), which state that the occurrence of severe droughts over the Middle East and central south Asia are associated with La Niña conditions and warm SST

over the western Pacific. In this study, not only drought occurrences, but also normal and wet occurrences are probabilistic modeled using SST climate indices.

A one-year-out cross-validation ordinal multiple regression model based on the $OND\_Niño4$ and OND_WPSSTA^d as predictor is reconstructed to evaluate the predicted categories. The computed confusion matrix of the cross-validated model is 30% for the misclassification error, which implies that the model identifies correctly categories in 70% times.

Like OND, ordinal regression models are developed for predicting probabilities of JFM SPI categories. The following ordinal regression model with minimum values of AIC (81.9) and residual deviance (75.9) is the best model for prediction JFM SPI categories.

$$logit\big(P(JFM\_SPI\_CAT \le j)\big) = \hat{\alpha}_{j0} + 1.4JFM\_EM\_SSTA^d, \qquad j = 1,2 \tag{10}$$

or

$$P(JFM\_SPI\_CAT \le j) = \frac{\exp(\hat{\alpha}_{j0}+1.4JFM\_EM\_SSTA^d)}{1+\exp(\hat{\alpha}_{j0}+1.4JFM\_EM\_SSTA^d)}, \qquad j = 1,2 \tag{11}$$

where $\hat{\alpha}_{10}$=-2 and $\hat{\alpha}_{20}$=1.77. The estimated t statistic value which is 1.79, indicating that the estimated coefficient of $JFM\_EM\_SSTA^d$ is statistically significant at 10% significance level. The surrogate residual diagnostic for this model indicates that the assumptions about the nature of the surrogate residual are met (Figures not shown). Therefore, SSTA variations over the eastern Mediterranean Sea is an important factor in prediction of JFM SPI categories. However, the SSTA variations over different parts of the Pacific Ocean are not related to JFM SPI categories in Iran (Table 3). The probabilistic prediction of JFM SPI categories using the fitted model based on the significant predictor are plotted in Fig. 4c. In JFM season, the chance of wet (dry) condition in Iran is low when SSTA over the eastern Mediterranean is in the warm (cold) phase (Fig. 4c). Using the confusion matrix, the misclassification error for the cross-validated model for JFM season is 41%, which is higher than found for OND.

4.3. Circulation characteristics affecting precipitation

We compare the OND and JFM circulation patterns to highlight why the same Niño indices are not teleconnected with JFM season. The anomalies data, which are computed by subtracting the climatological mean from the data, are considered here to evaluate the deviation from the long-term average. The low (850 hPa), mid (500 hPa), and upper level (200 hPa) atmospheric large scale circulation pattern anomalies during OND season for dry and wet conditions in Iran are shown in Figures 5, 6, and 7, respectively. During OND season for these conditions, the precipitable water anomalies also composited with vector winds anomalies are shown in Figure 5. By comparing Fig. 5a with Fig. 5b, it is observed that the wind directions are different for dry and wet OND seasons over Saudi Arabia, Iran and those areas which are important to supply the moisture for Iran. The main source of supplied moisture is mostly located over the southern and eastern water bodies such as Arabian and Oman Seas, Persian Gulf, Indian Ocean for OND precipitation over Iran. Fig. 5a and 5b also indicate that the amount of precipitable water anomalies during dry and wet OND season are, respectively, below- and above- normal over abovementioned source of moisture. Therefore, vector wind direction and amount of moisture over the above mentioned water bodies play important roles in dry and wet condition in Iran. The 850 hPa circulation patterns are connected with the 500 and 200 hPa circulation patterns (Fig. 6a, b and Fig. 7a,

b). The mid-level vector wind anomalies during dry (wet) OND season are outflow (inflow) over Iran (Fig. 6a, b). The 200 hPa upper level wind anomalies during dry (wet) OND seasons indicate easterly (westerly) wind at approximately 0-30N, which are associated with the changes in Rossby wave patterns (Glatt and Wirth 2014). On the other hand, previous studies (Niranjan Kumar and Ouarda 2014; Niranjan Kumar et al. 2016) reported that the Rossby wave pattern is related to ENSO. The composite map (Fig not shown) of vector wind at 850 hPa and PW anomalies for La Niña years is similar to Fig. 5a, because 6 out of the 7 coldest OND Niño3.4 SST anomalies are concurrent with dry OND conditions. These results support the physical mechanism that SSTA variations over the Pacific and Indian Oceans are important variables in the estimated ordinal regression equation to predict OND SPI categories.

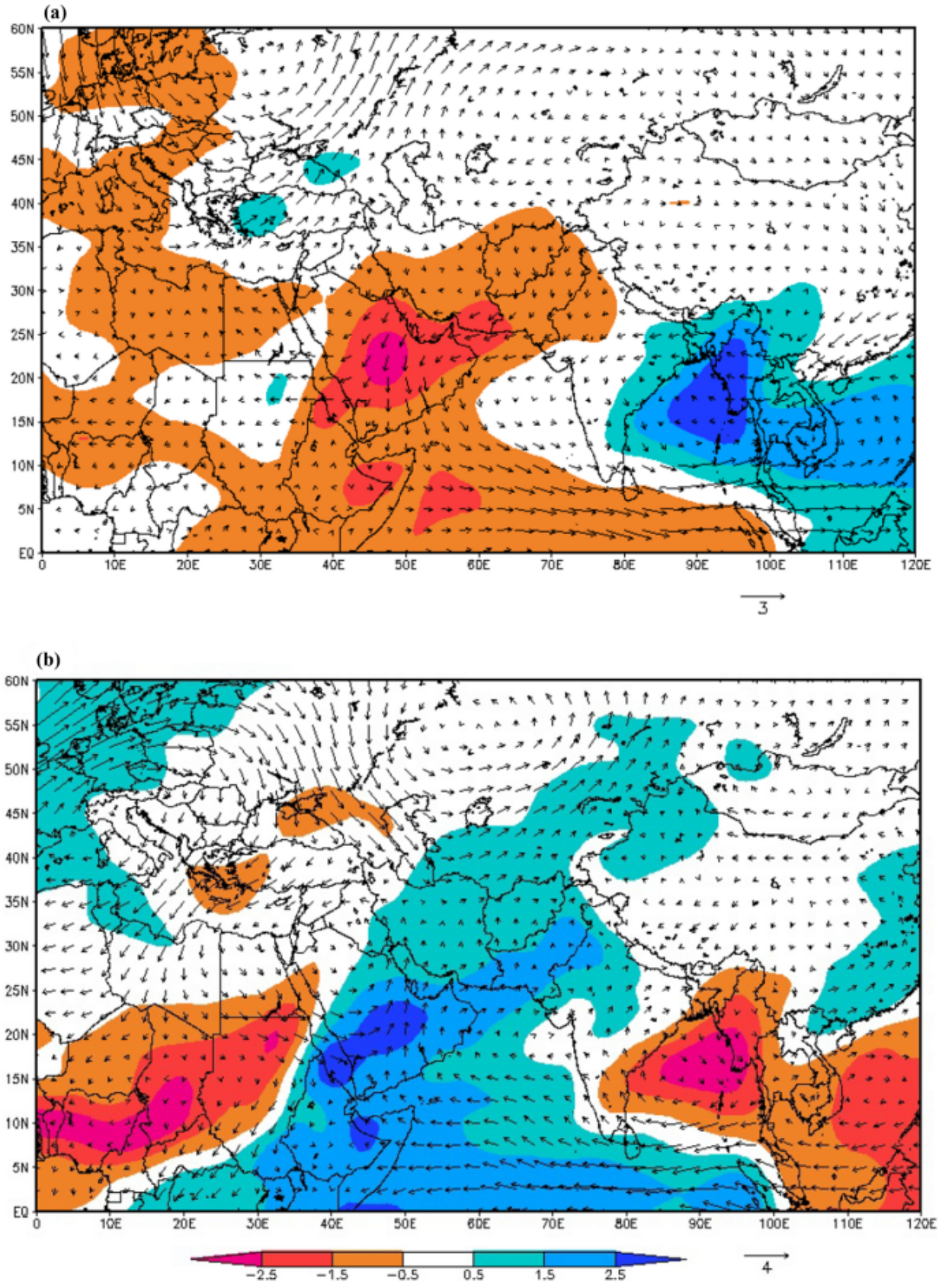

Figure 5. The composite maps of vector wind anomalies at 850 hPa and PW anomalies for dry (**a**) and wet (**b**) OND season

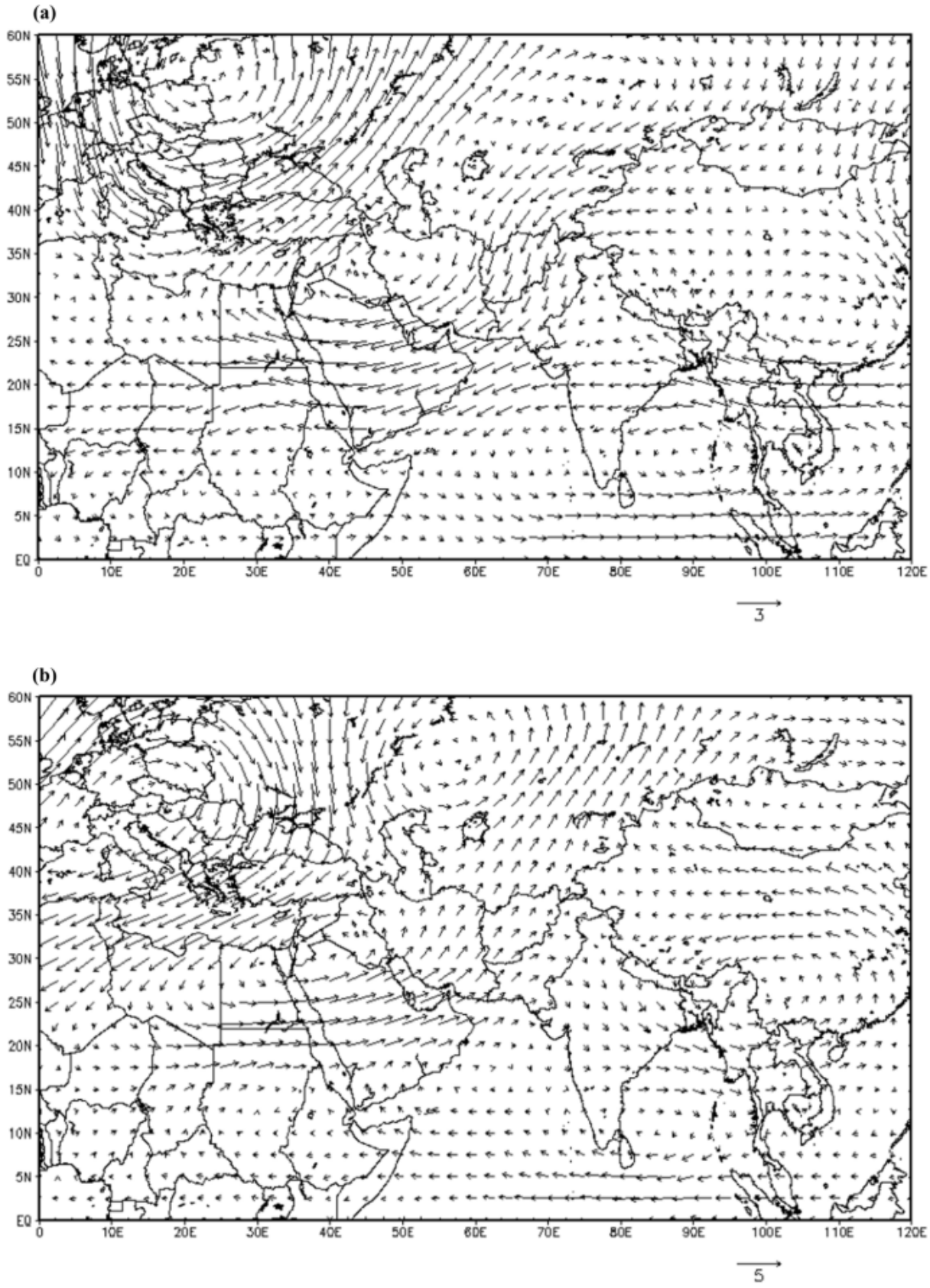

Figure 6. The vector wind anomalies at 500 hPa for dry (**a**) and wet (**b**) OND season

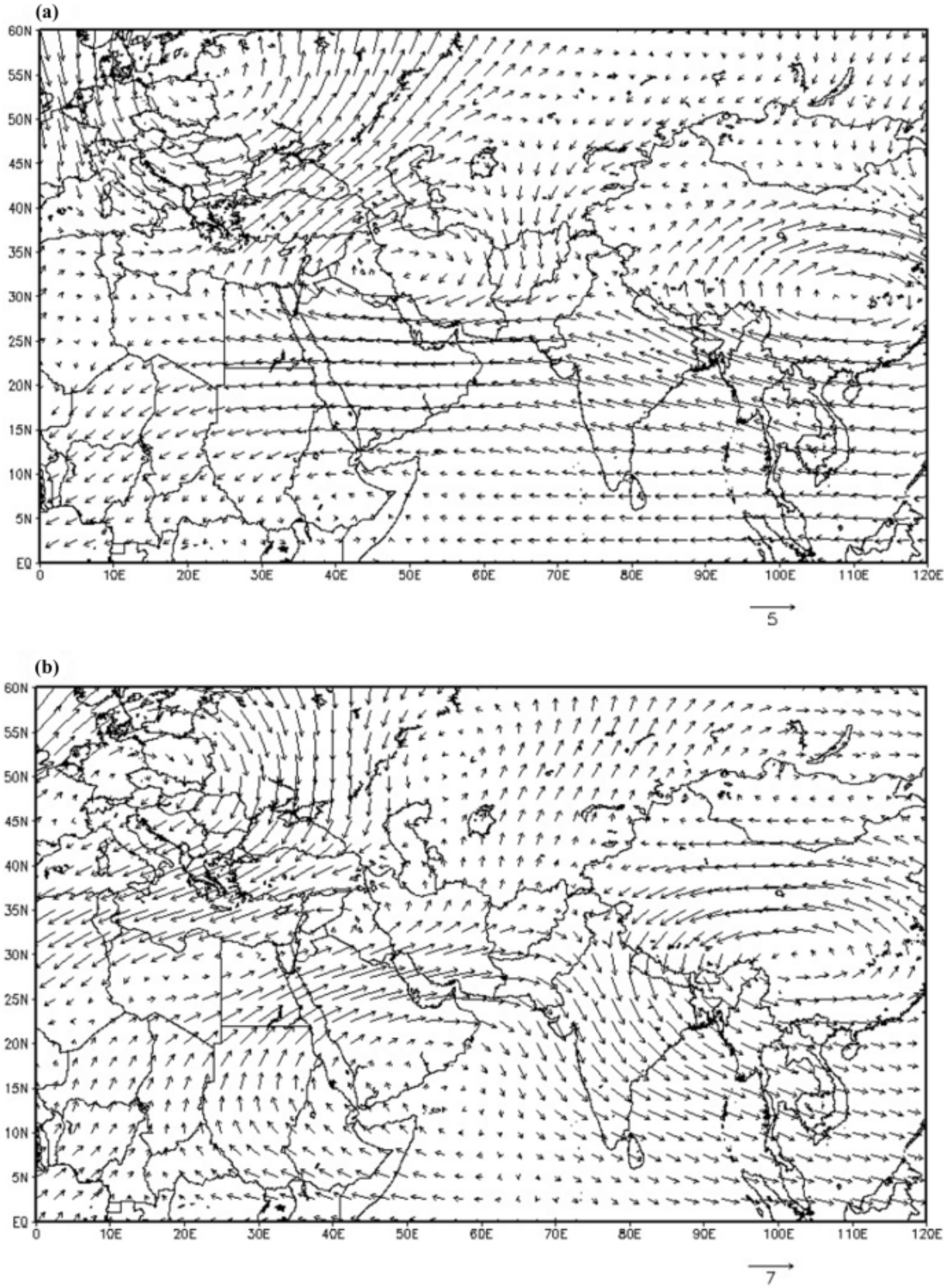

Figure 7. The vector wind anomalies at 200 hPa for dry (**a**) and wet (**b**) OND season

The composite map of 850 hPa vector wind and PW anomalies for dry and wet JFM seasons is shown in Fig. 8a, b. The wind flow over the northern parts of Africa, the Red Sea, and the eastern parts of the Mediterranean Sea transfers above-normal PW anomalies over these areas into Iran during wet JFM seasons (Fig. 8b). The wet JFM seasons in Iran are concurrent with the low-level cyclones between the eastern Mediterranean Sea and southern the black Sea-center over the Turkish- and a low-level anti-cyclone centered over the northeastern of the Indian Ocean (Fig. 8b). However, the wind has a southerly direction over the southwest of Iran and amount of PW anomalies is anomalously low during dry JFM seasons (Fig. 8). The dry JFM seasons are concurrent with a low-level anti-cyclone over the eastern Mediterranean Sea- centered over Iran and low-level cyclone centered over the Arabian Sea (Fig. 8a). These low-level patterns are connected with the 500 and 200 hPa circulation patterns (Figs. 9 and 10) such that a high (low) upper-level pressure - centered between the eastern Mediterranean Sea and Iran- is concurrent with dry (wet) JFM seasons in Iran. During dry (wet) JFM season, the mid-level vector wind anomalies are outflow (inflow) over Iran (Fig. 9a, b). Figure 11 (12) indicates areas in which the Pearson correlation between OND (JFM) precipitation over Iran and circulation patterns are significant at 5% level for the whole period. By comparing Figure 9 with Figure 10, it is seen that the areas in which the correlation is significant are different for OND and JFM seasons. These results suggest that –unlike OND seasons - from a synoptic perspective the role of circulation patterns over the Black and eastern Mediterranean Sea and also moisture over these areas and north of Africa are important for dry and wet JFM seasons in Iran.

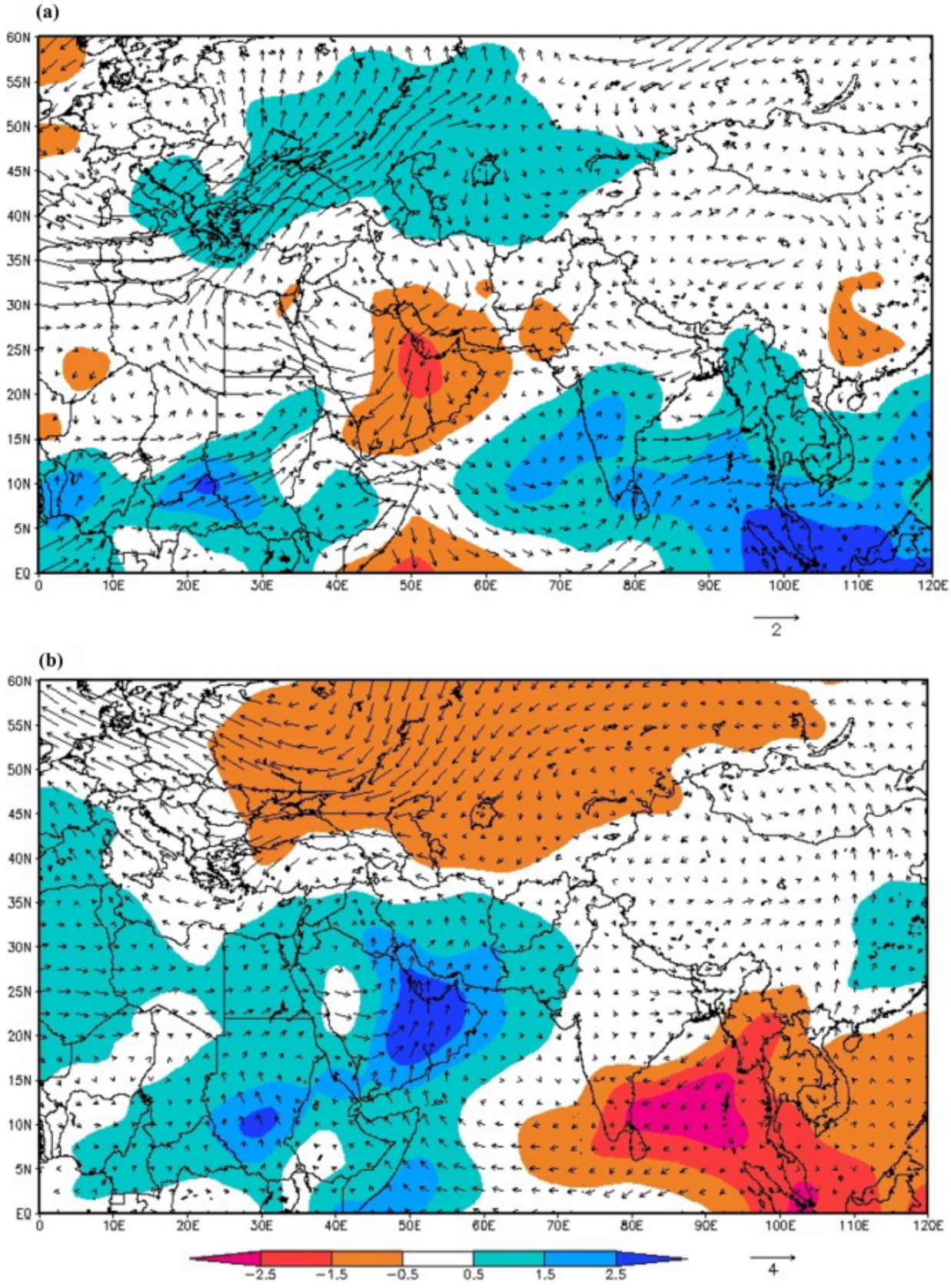

Figure 8. The composite maps of vector wind anomalies at 850 hPa and PW anomalies for dry (**a**) and wet (*b*) JFM season

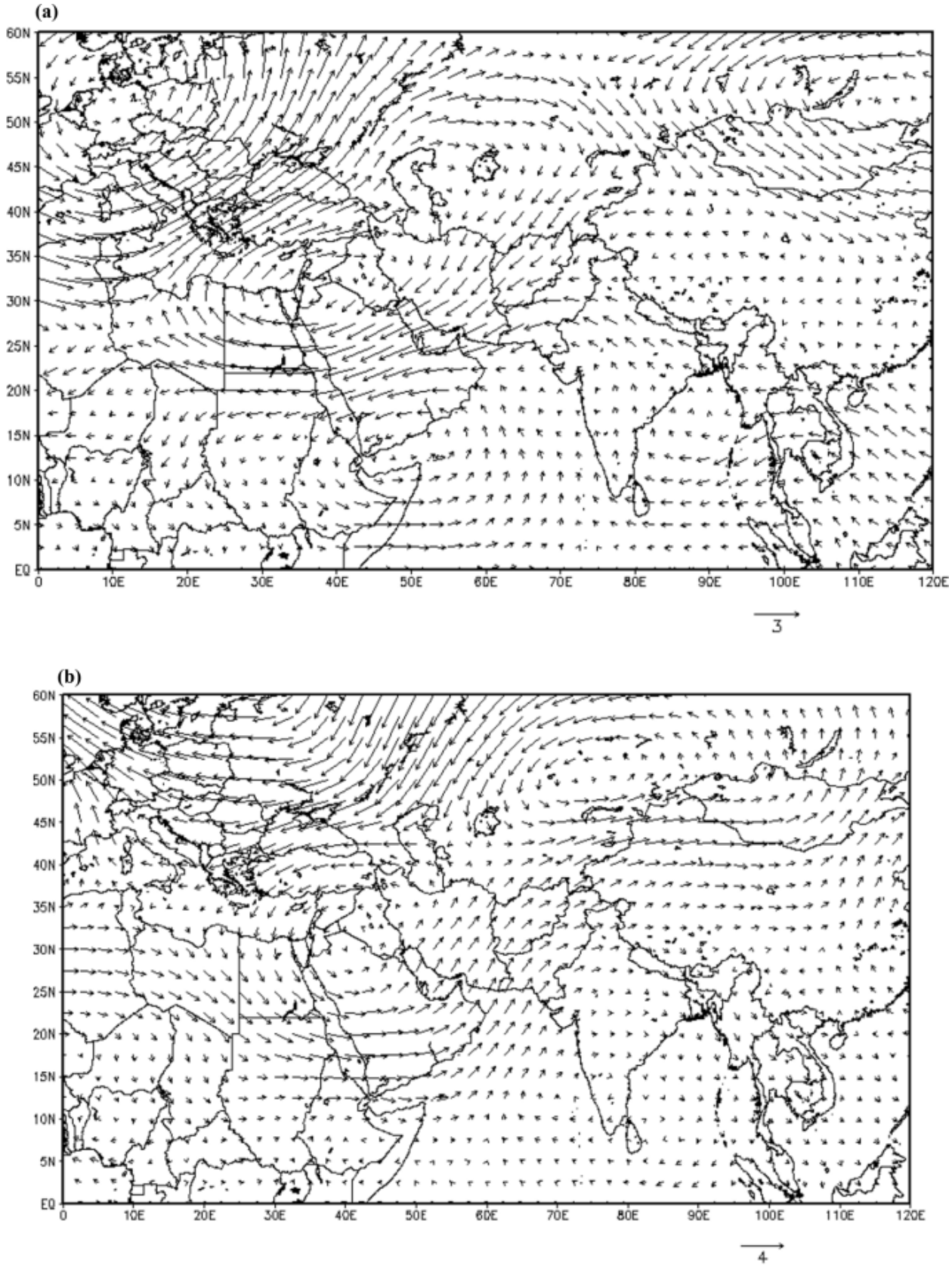

Figure 9. The vector wind anomalies at 500 hPa for dry (**a**) and wet (**b**) JFM season

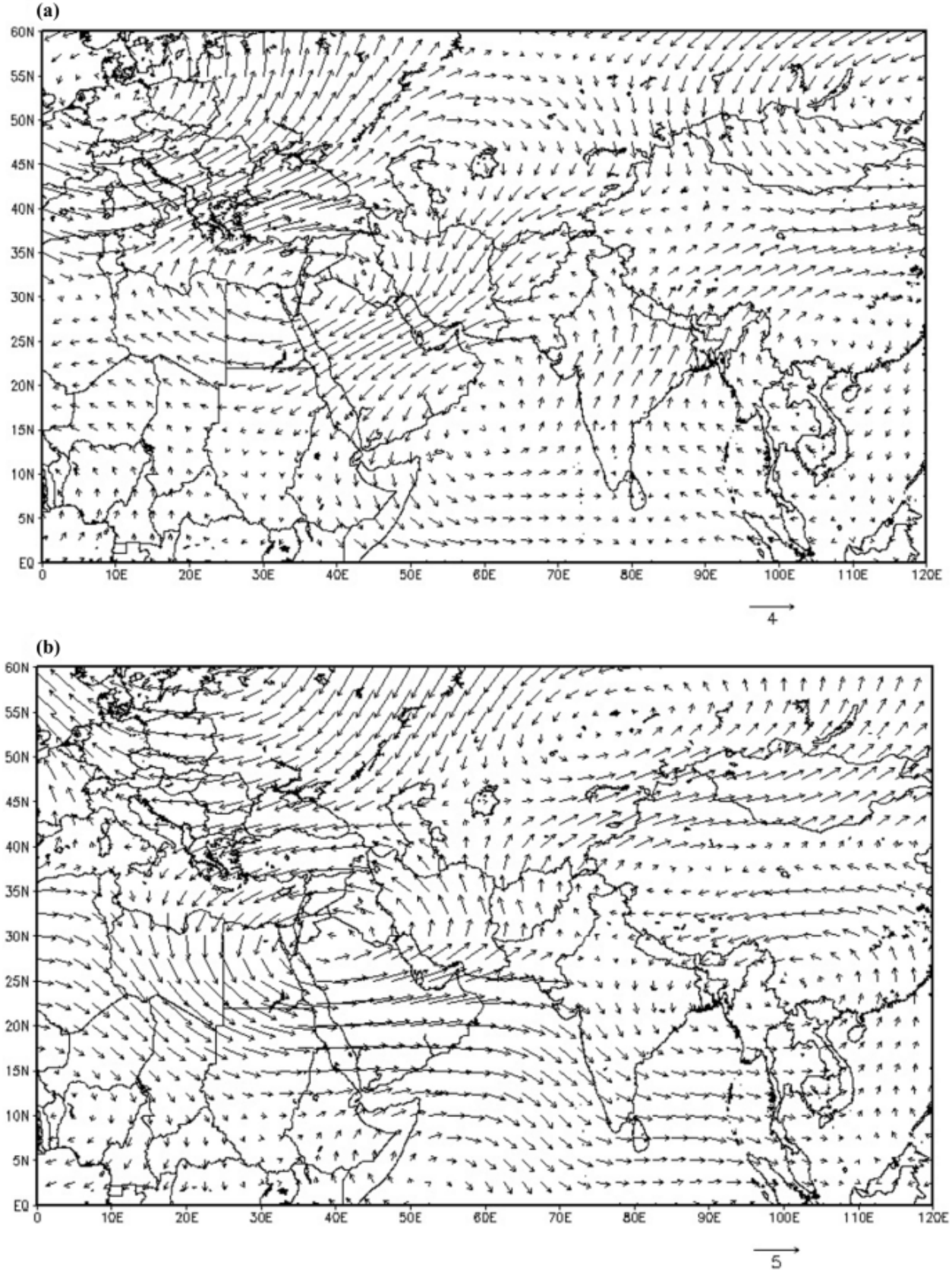

Figure 10. The vector wind anomalies at 200 hPa for dry (**a**) and wet (**b**) JFM season

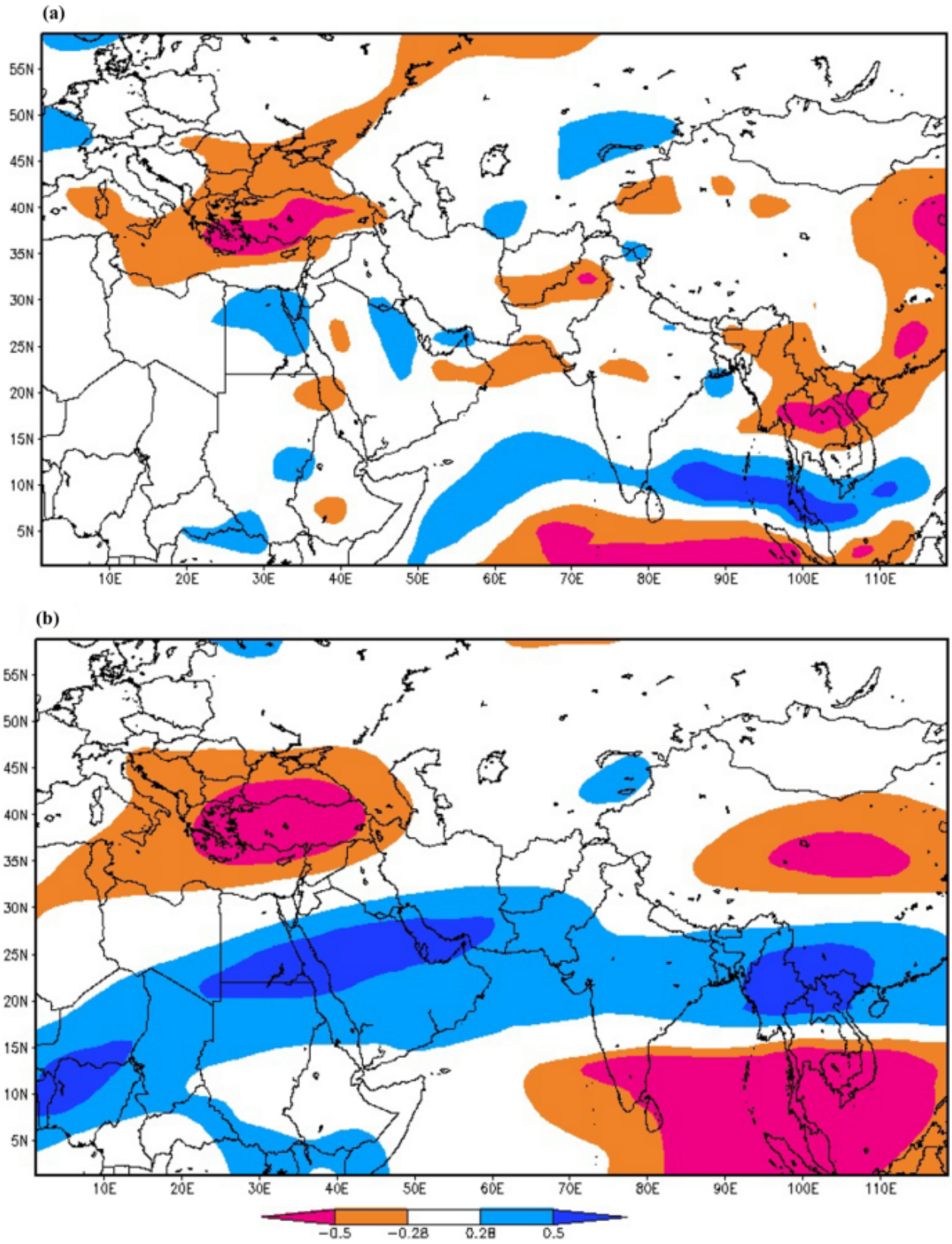

Figure 11. The Pearson correlation maps of 850 (**a**) and 200 (**b**) hPa wind magnitude with OND precipitation over Iran. White parts indicate non-significant area

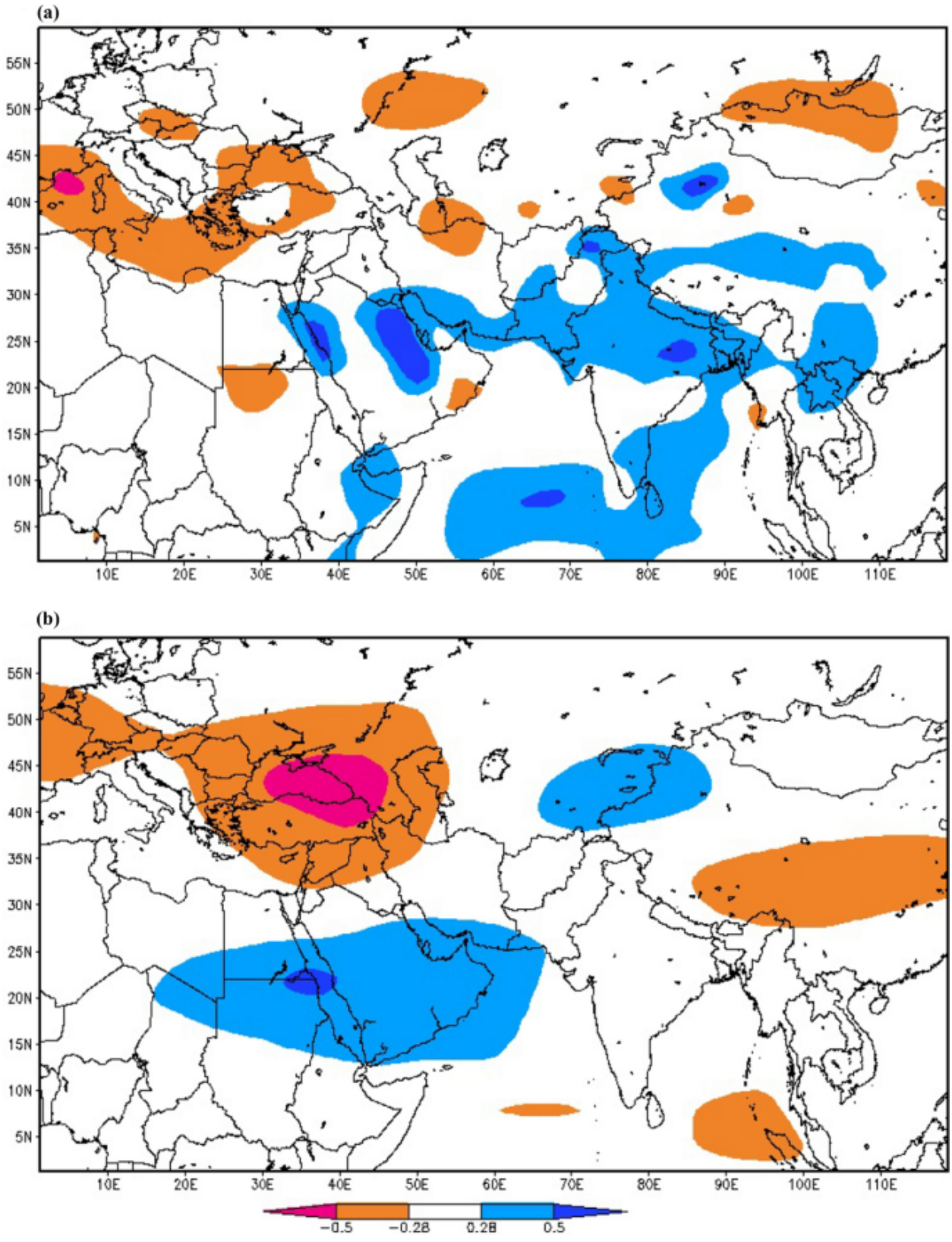

Figure 12. Iran. White parts indicate non-significant area

5. Summary and Conclusions

The teleconnection between the SST climate indices and seasonal SPI categories over Iran has been examined using state-of-the-art ordinal regression models. These models were constructed over a long period of observed precipitation and SSTA datasets. Those time series (such as JFM SPI values, EMSTA) which indicated a significant trend, were subsequently de-trended before constructing ordinal regression models. In this manner, the variations of SPI categories are realistically connected by climate indices through the models and the established teleconnections are reliable and also the assumptions of regression models will be met.

The time series of OND and JFM SPI values over Iran indicate a non-significant and significant downward trend over a long period, respectively. This result suggests that the risk of drought in the JFM season has been enhanced in Iran. The NAO and oceanic indices over the tropical Pacific-including Niño4, Niño3.4, Niño3, Niño1+2-, western Pacific, and Indian Ocean are each significant in their own right for predicting the OND SPI categories. Moreover, the Niño3.4 and WP produces the best combined indices for estimating probabilities of wet and dry OND seasons. Among all predictors in the ordinal regression models, the SST anomalies variations over the eastern Mediterranean Sea are teleconnected significantly with JFM SPI categories. Therefore, unlike OND seasons, the SST anomalies over different parts of the Pacific Ocean are not strongly related to JFM seasons in Iran. Probabilistic drought prediction, which is important and popular for decision making, over Iran has been modeled and the relationships between SSTA and drought can be explained using the ordinal regression models. The OND circulation patterns in Section 4.3 explain why SSTA variations over the Pacific and Indian Oceans are important variables for predicting OND SPI categories, that is Black and Mediterranean Seas for JFM. The mid and upper level vector wind is causes outflow of moisture over Iran during dry seasons, and inflow of moisture for wet seasons.

Acknowledgment

The authors greatly appreciate the two anonymous reviewers for their suggestions which led to improvements in the manuscript.

Data availability

The precipitation data set were obtained from http://www.irimo.ir/. The ERSSTA, reanalysis specific humidity, zonal and meridional components of wind were downloaded from IRI data library https://iridl.ldeo.columbia.edu/.

Apart from that–the datasets generated during and/or analyzed during the current study are available from the corresponding author on reasonable request.

References

Agrawala S, Barlow M, Cullen H, Lyon B (2001) The drought and humanitarian crisis in central and southwest Asia: A climate perspective IRI Special Report NO 01-11:20-20 doi:10.7916/D8NZ8FHQ

Al Senafi F, Anis A (2015) Shamals and climate variability in the Northern Arabian/Persian Gulf from 1973 to 2012 International Journal of Climatology 35:4509-4528 doi:10.1002/joc.4302

Alizadeh-Choobari O, Adibi P, Irannejad P (2018) Impact of the El Niño–Southern Oscillation on the climate of Iran using ERA-Interim data Climate Dynamics 51:2897-2911 doi:10.1007/s00382-017-4055-5

Athar H (2015) Teleconnections and variability in observed rainfall over Saudi Arabia during 1978-2010 Atmospheric Science Letters 16:373-379 doi:10.1002/asl2.570

Balmaseda M, Anderson D (2009) Impact of initialization strategies and observations on seasonal forecast skill Geophysical Research Letters 36:L01701-L01701 doi:10.1029/2008GL035561

Barlow M, Cullen H, Lyon B (2002) Drought in Central and Southwest Asia: La Niña, the Warm Pool, and Indian Ocean Precipitation Journal of Climate 15:697-700 doi:10.1175/1520-0442(2002)015<0697:DICASA>2.0.CO;2

Barlow M, Hoell A (2015) Drought in the Middle East and Central–Southwest Asia During Winter 2013/14 Bulletin of the American Meteorological Society 96:S71-S76 doi:10.1175/BAMS-D-15-00127.1

Barlow M, Hoell A, Agel L (2021) An evaluation of CMIP6 historical simulations of the cold season teleconnection between tropical Indo-Pacific sea surface temperatures and precipitation in Southwest Asia, the coastalMiddle East , and Northern Pakistan and India. J Climate, doi:10.1175/JCLI-D-19-1026.

Bazrkar MH, Chu X (2022) Development of category-based scoring support vector regression (CBS-SVR) for drought prediction. Journal of Hydroinformatics 24(1): 202-222 doi:10.2166/hydro.2022.104

Bilder CR (2014) Analysis of Categorical Data with R. Chapman and Hall/CRC. doi:10.1201/b17211

Demargne J, Wu L, Regonda SK, Brown JD, Lee H, He M, Seo DJ, Hartman R, Herr HD, Fresch M, Schaake J (2014) The science of NOAA's operational hydrologic ensemble forecast service. Bulletin of the American Meteorological Society, 95(1):9-98.

Glickman, T.S., 2000. Glossary of meteorology. American Meteorological Society.

Glatt I, Wirth V (2014) Identifying Rossby wave trains and quantifying their properties Quarterly Journal of the Royal Meteorological Society 140:384-396 doi:10.1002/qj.2139

Goddard L, Dilley M (2005) El Niño: Catastrophe or Opportunity Journal of Climate 18:651-665 doi:10.1175/JCLI-3277.1

Hao Z, Hong Y, Xia Y, Singh VP, Hao F, Cheng H (2016) Probabilistic drought characterization in the categorical form using ordinal regression Journal of Hydrology 535:331-339 doi:10.1016/j.jhydrol.2016.01.074

Hoell A, Barlow M, Saini R (2012) The Leading Pattern of Intraseasonal and Interannual Indian Ocean Precipitation Variability and Its Relationship with Asian Circulation during the Boreal Cold Season Journal of Climate 25:7509-7526 doi:10.1175/JCLI-D-11-00572.1

Hoell A, Funk C, Barlow M (2014a) La Niña diversity and Northwest Indian Ocean Rim teleconnections Climate Dynamics 43:2707-2724 doi:10.1007/s00382-014-2083-y

Hoell A, Funk C, Barlow M (2014b) The regional forcing of Northern hemisphere drought during recent warm tropical west Pacific Ocean La Niña events Climate Dynamics 42:3289-3311 doi:10.1007/s00382-013-1799-4

Hoell A, Shukla S, Barlow M, Cannon F, Kelley C, Funk C (2015) The Forcing of Monthly Precipitation Variability over Southwest Asia during the Boreal Cold Season Journal of Climate 28:7038-7056 doi:10.1175/JCLI-D-14-00757.1

Huang B et al. (2017) Extended Reconstructed Sea Surface Temperature, Version 5 (ERSSTv5): Upgrades, Validations, and Intercomparisons Journal of Climate 30:8179-8205 doi:10.1175/JCLI-D-16-0836.1

Kalnay E et al. (1996) The NCEP/NCAR 40-Year Reanalysis Project Bulletin of the American Meteorological Society 77:437-471 doi:10.1175/1520-0477(1996)077<0437:TNYRP>2.0.CO;2

Karimi, M., Melesse, A.M., Khosravi, K., Mamuye, M. and Zhang, J., 2019. Analysis and prediction of meteorological drought using SPI index and ARIMA model in the Karkheh River Basin, Iran. In Extreme Hydrology and Climate Variability (pp. 343-353). Elsevier.

Krichak SO, Breitgand JS, Gualdi S, Feldstein SB (2014) Teleconnection–extreme precipitation relationships over the Mediterranean region Theoretical and Applied Climatology 117:679-692 doi:10.1007/s00704-013-1036-4

Landman WA, Barnston AG, Vogel C, Savy J (2019) Use of El Niño–Southern Oscillation related seasonal precipitation predictability in developing regions for potential societal benefit International Journal of Climatology 39:5327-5337 doi:10.1002/joc.6157

Landman WA, Beraki A (2012) Multi-model forecast skill for mid-summer rainfall over southern Africa International Journal of Climatology 32:303-314 doi:10.1002/joc.2273

Liu D, Zhang H (2018) Residuals and Diagnostics for Ordinal Regression Models: A Surrogate Approach Journal of the American Statistical Association 113:845-854 doi:10.1080/01621459.2017.1292915

Mariotti A (2007) How ENSO impacts precipitation in southwest central Asia Geophysical Research Letters 34 doi:10.1029/2007GL030078

Mason SJ, Goddard L (2001) Probabilistic Precipitation Anomalies Associated with ENSO Bulletin of the American Meteorological Society 82:619-638 doi:10.1175/1520-0477(2001)082<0619:PPAAWE>2.3.CO;2

McKee TB, Doesken NJ, Kleist J The relationship of drought frequency and duration to time scales. In, 1993 1993. American Meteorological Society Boston, MA, pp 179-183

Nazemosadat MJ, Cordery I (2000) On the relationships between ENSO and autumn rainfall in Iran International Journal of Climatology 20:47-61 doi:10.1002/(SICI)1097-0088(200001)20:1<47::AID-JOC461>3.0.CO;2-P

Nazemosadat MJ, Ghasemi AR (2004) Quantifying the ENSO-related shifts in the intensity and probability of drought and wet periods in Iran Journal of Climate 17:4005-4018 doi:10.1175/1520-0442(2004)017<4005:QTESIT>2.0.CO;2

Niranjan Kumar K, Ouarda TBMJ (2014) Precipitation variability over UAE and global SST teleconnections Journal of Geophysical Research: Atmospheres 119:10,313-310,322 doi:10.1002/2014JD021724

Niranjan Kumar K, Ouarda TBMJ, Sandeep S, Ajayamohan RS (2016) Wintertime precipitation variability over the Arabian Peninsula and its relationship with ENSO in the CAM4 simulations Climate Dynamics 47:2443-2454 doi:10.1007/s00382-016-2973-2

Price C, Stone L, Huppert A, Rajagopalan B, Alpert P (1998) A possible link between El Nino and precipitation in Israel Geophysical Research Letters 25:3963-3966 doi:10.1029/1998GL900098

Rana S, Renwick J, McGregor J, Singh A (2018) Seasonal Prediction of Winter Precipitation Anomalies over Central Southwest Asia: A Canonical Correlation Analysis Approach Journal of Climate 31:727-741 doi:10.1175/JCLI-D-17-0131.1

Raziei T. Bordi I, Pereira LS, Corte-Real J, Santos JA (2012) Relationship between daily atmospheric circulation types and winter dry/wet spells in western Iran. International Journal of Climatology 32(7):1056-1068 doi:10.1002/joc.2330.

Shirvani A, Landman WA (2016) Seasonal precipitation forecast skill over Iran International Journal of Climatology 36:1887-1900 doi:10.1002/joc.4467

Svoboda M, Hayes M, Wood D (2012) Standardized precipitation index user guide World Meteorological Organization Geneva, Switzerland

Syed FS, Giorgi F, Pal JS, King MP (2006) Effect of remote forcings on the winter precipitation of central southwest Asia part 1: observations Theoretical and Applied Climatology 86:147-160 doi:10.1007/s00704-005-0217-1

Trenberth KE, Fasullo J, Smith L (2005) Trends and variability in column-integrated atmospheric water vapor. Climate dynamics 24(7):741-758 doi:10.1007/s00382-005-0017-4

Weisheimer A et al. (2009) ENSEMBLES: A new multi-model ensemble for seasonal-to-annual predictions—Skill and progress beyond DEMETER in forecasting tropical Pacific SSTs Geophysical Research Letters 36:L21711-L21711 doi:10.1029/2009GL040896

Wilks DS (2011) Statistical methods in the atmospheric sciences. Academic Press, San Diego, CA

Yin Z-Y, Wang H, Liu X (2014) A Comparative Study on Precipitation Climatology and Interannual Variability in the Lower Midlatitude East Asia and Central Asia Journal of Climate 27:7830-7848 doi:10.1175/JCLI-D-14-00052.1

Zarei AR, Moghimi MM, Bahrami M (2017) Monitoring and prediction of monthly drought using Standardized Precipitation Index and Markov Chain (Case study: southeast of Iran). Geography and Environmental Sustainability, 7(2): 39-51.